

This is an Open Access document downloaded from ORCA, Cardiff University's institutional repository: <https://orca.cardiff.ac.uk/id/eprint/66815/>

This is the author's version of a work that was submitted to / accepted for publication.

Citation for final published version:

Hazelwood, Tobias, Jefferson, Anthony Duncan , Lark, Robert John and Gardner, Diane Ruth 2014. Long-term stress relaxation behavior of predrawn poly(ethylene terephthalate). *Journal of Applied Polymer Science* 131 (23) , 41208. 10.1002/app.41208

Publishers page: <http://dx.doi.org/10.1002/app.41208>

Please note:

Changes made as a result of publishing processes such as copy-editing, formatting and page numbers may not be reflected in this version. For the definitive version of this publication, please refer to the published source. You are advised to consult the publisher's version if you wish to cite this paper.

This version is being made available in accordance with publisher policies. See <http://orca.cf.ac.uk/policies.html> for usage policies. Copyright and moral rights for publications made available in ORCA are retained by the copyright holders.



# **Long-term stress relaxation behaviour of pre-drawn PET**

T. Hazelwood,<sup>1</sup> A. D. Jefferson,<sup>1</sup> R.J. Lark,<sup>1</sup> D. R. Gardner<sup>1</sup>

<sup>1</sup>Cardiff School of Engineering, Cardiff University, Queen's Buildings, The Parade, Cardiff, CF24 3AA, Wales, UK

Correspondence to: T. Hazelwood (hazelwoodt@cf.ac.uk).

## **ABSTRACT**

Research has been carried out with the aim of better understanding the relevant properties of materials to be used in a new self-healing cementitious composite material system. In a previous study the build-up of stress in a heat-activated restrained pre-drawn poly(ethylene terephthalate) (PET) specimen was investigated. In the current study, the long-term stress relaxation behaviour of such a restrained specimen has been explored so that its potential for use in the new material system can be better understood. The work includes an experimental study in which the stress in a number of PET specimens, restrained against longitudinal shrinkage, was measured during the initial heat activation and cooling phases, and then monitored for a further 6 months. These data were used to quantify the stress relaxation of the specimen and inform the development of a new one dimensional numerical model to simulate the thermo-mechanical behaviour of this material. This model is shown to be able to reproduce the observed short and long-term experimental behaviour with good accuracy.

## **KEYWORDS**

Mechanical properties, theory and modelling, thermal properties, viscosity and viscoelasticity

## INTRODUCTION

This paper considers the short and long-term behaviour of activated pre-drawn PET tendons in the context of a new material system named LatconX. This system comprises SMP tendons embedded within a cementitious matrix, along with the required reinforcing steel. The shrinkage process of these tendons would then be activated at a certain point in time to provide a compressive force to the cementitious matrix. It has been shown that this compressive force serves three purposes: closing any cracks that have developed; applying a compressive stress to the cracked faces leading to improved self-healing of the cracks; and improving the structural performance of the composite system by acting in the same manner as a prestressing system. This system has been described in more detail by Jefferson et al.<sup>1</sup>

A detailed understanding of the long-term behaviour of the pre-drawn PET tendons is vital to continued development of the LatconX system; the research presented in this publication aims to address this knowledge gap through a combination of experimental and numerical studies.

Recent constitutive modelling work undertaken in the area of shape memory polymers has focused on the programming of the shape memory effect and the material's behaviour immediately before and after activation. An early approach developed by Pakula and Trznadel<sup>2</sup> accounted for the temperature dependence of amorphous polymers by use of a four-state model. The model which consists of two elastic springs and two two-site elements is capable of qualitatively representing the temperature dependence of shrinkage forces in these materials. Morshedian et al<sup>3</sup> developed this model further by replacing the two-site elements with temperature-dependent dashpots leading to a good fit with experimental results. Dunn et al<sup>4</sup>

investigated the short term restrained stress development of pre-drawn PET. A one dimensional numerical model based on Zener's standard linear solid model was developed with the aid of an experimental study, with the model being validated using a further data set and shown capable of predicting the initial stress build up behaviour of restrained pre-drawn PET.

A different approach to the modelling of the shape memory phenomenon is to consider the polymer as consisting of a number of distinct phases each with its own material properties and constitutive relationship. An example of this type of model is the work of Liu et al,<sup>5</sup> the model consists of rubbery and frozen phases which account for the differences in state either side of the glass transition. The contribution of each of these phases to the overall material behaviour at any instant is a function of temperature. Barot and coworkers<sup>6,7</sup> have developed a model based on these principles for the shape memory effect; two phases are used to represent the different material states, rubbery amorphous and rigid semi-crystalline, with the crystallising and melting processes governed by prescribed rate equations. Qi et al<sup>8</sup> take these concepts further in the development of a three-dimensional model in which the glassy phase considered by Liu et al<sup>5</sup> is divided into a frozen glassy phase and an initial glassy phase in order to account for the glassy phase's deformation history.

A considerable volume of research into the long-term viscoelastic behaviour of polymers exists.

Ward and Sweeney<sup>9</sup> discussed three well known phenomenological models; namely Kelvin, Maxwell, and standard linear solid (SLS) models. These models are useful in modelling linear behaviour of viscoelastic materials such as pre-drawn PET.

Wang et al<sup>10</sup> studied the behaviour of Nylon films subject to constant rate compression, with an SLS model being used to accurately describe the viscoelastic behaviour of the films. Almagableh et al,<sup>11</sup> demonstrated the use of an SLS model to predict the viscoelastic behaviour of vinyl ester nanocomposites. In this work samples of vinyl ester were subjected to both creep and relaxation tests at a range of temperatures and the SLS model is shown to be capable of accurately simulating the measured behaviour.

Other methods for the prediction of long-term viscoelastic behaviour, besides the linear models mentioned above, include; a model for the long-term viscoelastic behaviour of aging polymers based on the concept of transient chain networks.<sup>12</sup> In this investigation, constitutive equations were derived by treating a viscoelastic medium as a system of adaptive links. The adjustable parameters were set using short term creep and relaxation tests and the model validated by comparison with experimental data.

Xu and Hou<sup>13</sup> presented a stress relaxation model based on the assumption that creep and stress relaxation are functions of a single physical phenomenon. A new stress relaxation relationship was derived and shown to agree closely with experimental data for a wide range of viscoelastic materials.

The motivation for the present study is the need to accurately predict the long-term stress relaxation behaviour of a shape memory polymer subjected to thermally activated restrained shrinkage and this is a matter not directly addressed in previous investigations.

A thermodynamic inconsistency with the model presented by Dunn et al<sup>4</sup> has also been addressed in the development of the new model. This inconsistency arises

from the temperature dependency of the Young's modulus of the polymer, which increases as the temperature decreases after thermal activation.

In this study, an experimental test series investigating the stress relaxation behaviour of pre-drawn PET is presented. The form of a new constitutive model is described and its solution explained. Finally, techniques for determining the model parameters are discussed and the model's ability to simulate viscoelastic behaviour is demonstrated.

## **EXPERIMENTAL**

A key element of this study was a series of experimental tests on the polymeric material. Data from these tests could then be used to calibrate the constitutive model as described later.

### **Material**

All experiments have been carried out using the drawn polymeric material Aerovac ShrinkTite, in 32 mm × 0.046 mm tape form. This was obtained from Aerovac (<http://www.aerovac.com/>), however the company has since changed name to Umeco (<http://www.umeco.com>).

### **Test Specimen Preparation**

All test specimens consisted of a number of strips of the polymer tape 400 mm long ( $\pm 2$ mm), clamped at both ends between steel plates that act as grips (see figure 1).

The number of strips varied from 8 to 25 depending on the exact conditions required for the test i.e. the stress required in the specimen.

Test specimens were held by a grip at each end consisting of two flat metal plates measuring 60 mm × 23 mm × 2 mm as shown in figure 1, these flat plates were held together by two bolts which could be tightened to hold the specimen in place.



**Figure 1 – Grip used to hold ends of test specimens**

It was important to ensure that the strips making up each specimen were all the same length between the two grips so that when any strain was applied the stress would be effectively equal in each strip. This was achieved by using a timber jig to hold the strips together along their full length while the end grips were attached.

Two types of stress relaxation tests were carried out on the polymer specimens, namely heat activated stress, and load induced stress tests.

### **Heat Activated Stress**

In the first category of tests, the specimen was held in the grips in a position so that it was just taut, a heat of 90°C was then applied to the specimen for a period of ten minutes, thus activating the shrinkage behaviour of the drawn polymer, and thereby inducing a stress within the specimen. This stress was monitored and logged over time as well as the ambient temperature of the surrounding environment. The experimental setup for this test is shown in figure 2.



**Figure 2 – Experimental setup for heat activated stress relaxation tests**

To enable these tests to be undertaken, an Instron oven was fixed within a Mechtronic reaction frame, fixings were constructed to connect the grips holding the specimen to the top and bottom of the reaction frame with the specimen running through the middle of the oven. A load cell was incorporated into these fixings above the oven as can be seen in figure 2. The force in the specimen, and the temperature at different locations both inside and outside the oven were monitored by a 2.5 kN load cell and 12 thermocouples respectively. These were all attached to a data logger with readings taken every 12 hours for the duration of the test.

Five of these tests have been carried out with a typical set of results being as presented in figure 3. From this it can be seen that the stress reaches a peak of 32.8 MPa at the start of the test before reducing over a period of approximately 100 days to an average plateau stress of 31.50 MPa. This value is an average since the stress continues to fluctuate between approximately 32 MPa and 31 MPa once the plateau is reached.

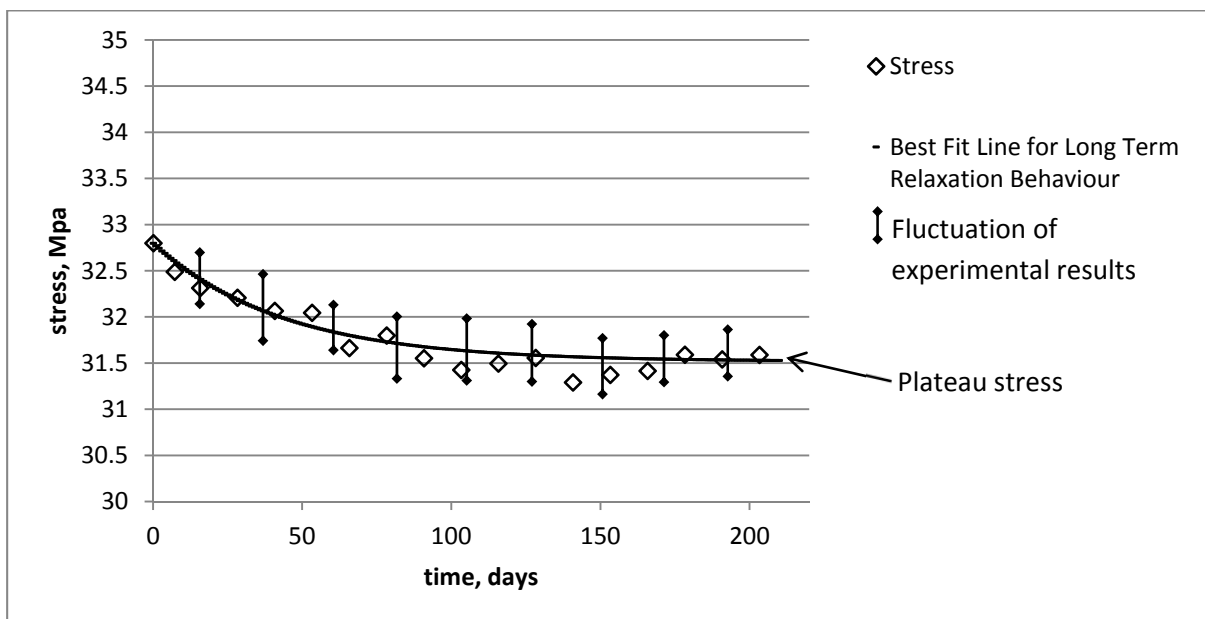


**Figure 3 – Normalised stress vs time for heat activated stress relaxation test**

The peak stress reached in these five tests has been observed to vary from a minimum of 26.0 MPa to a maximum of 32.8 MPa. Although the same specification of material was employed for all the tests, different rolls of material were used, and these peak stress differences are believed to relate to the variations in the supplied material. One theory is that the value of the peak stress is closely linked to the age of the material as the locked in stress is thought to gradually release over time. The length of time that the material relaxed over was also seen to vary, the maximum period was approximately 100 days, and the minimum was approximately 1 day; this tended to be a shorter time in the older material. Finally the plateau stress also

varied from a minimum of 96.4 % of the peak stress to a maximum of 98.6 % of the peak.

Due to the long time period required to carry out a test such as the one above, it was not possible to continue every test for this period. However four other shorter term tests were undertaken to confirm that a similar early trend was seen. These tests were found to show close agreement; they have been normalised to the peak stress and averaged to produce the results shown in figure 4.

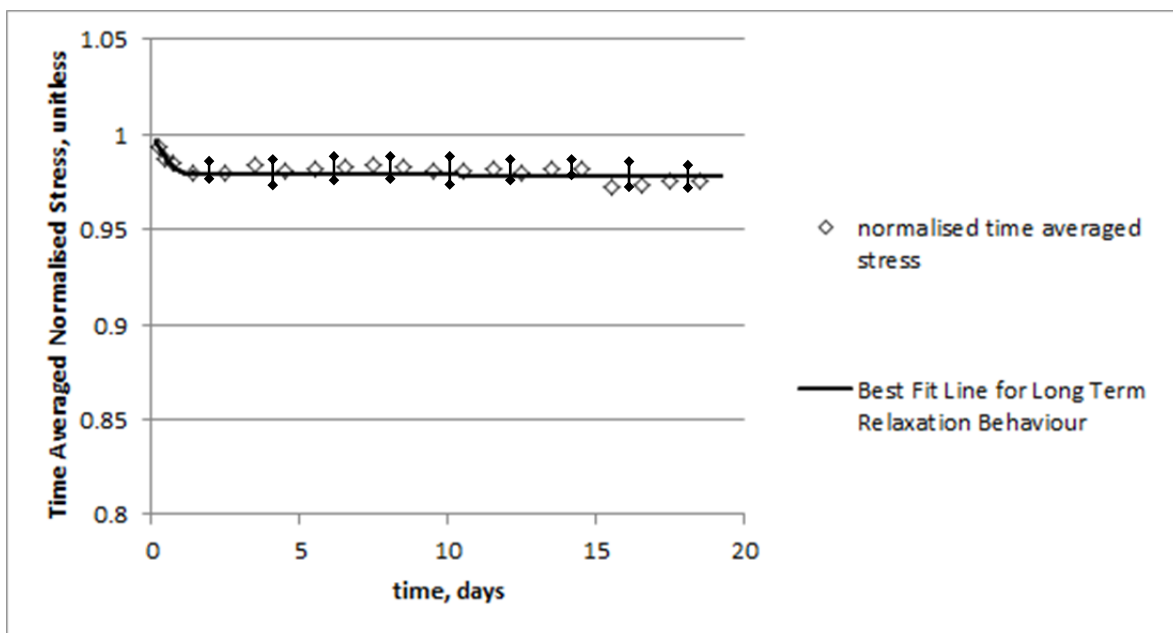
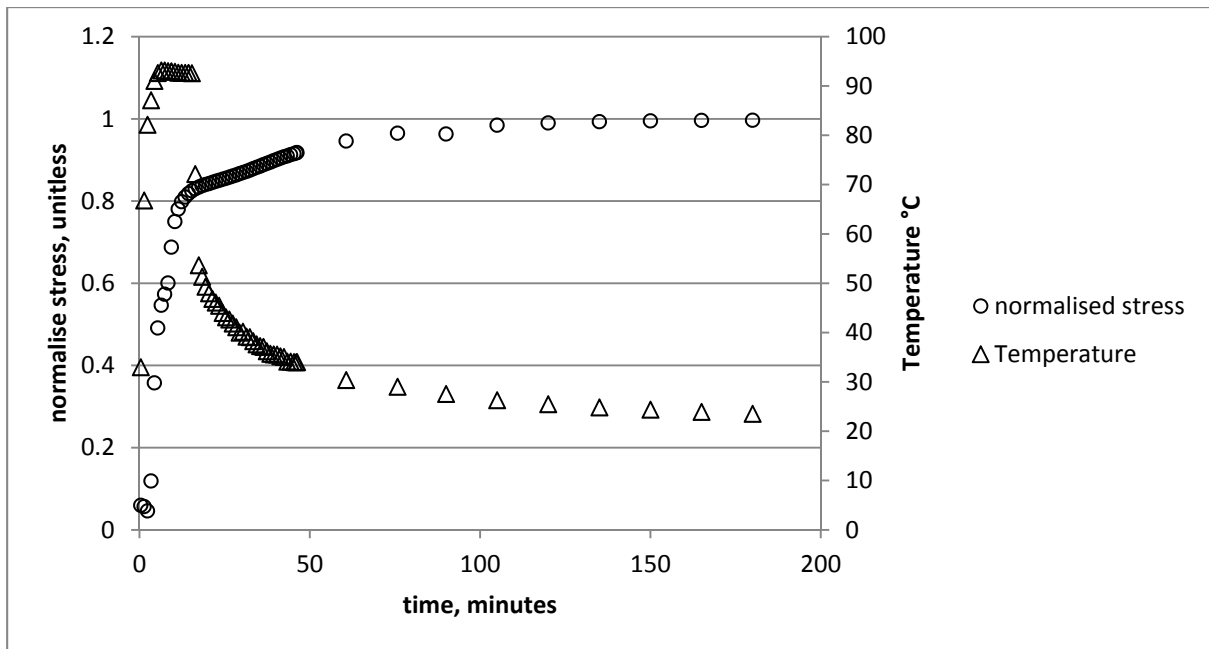


Figure 4 – Normalised average stress vs time for 4 different heat activated stress relaxation tests

Figure 4 shows the stress build up in the specimens upon heating and the subsequent relaxation to the plateau at 97.3% of the peak stress.



**Figure 5 - Normalised average stress vs time for 4 different heat activated stress relaxation tests (early stage only)**

Figure 5 shows the stress build up process during the first 200 minutes of testing in more detail; an initial stress decrease due to thermal expansion is observed followed by a sharp stress increase as the applied temperature enters the transition zone in which the drawn shrinkage process is activated. As the locked in stress is released, the rate of stress increase decreases and the stress begins to plateau. The rate of stress development increases again when the applied temperature is removed, causing thermal contraction of the specimen. Finally, as the temperature reaches ambient, the stress increase due to thermal contraction halts, and the stress again plateaus as all available locked in stress has been released.

The set of experimental results presented above have good implications for the use of this material in the proposed LatConX system as they show very limited stress relaxation. This is beneficial for two reasons; firstly it means that an adequate stress will be applied to the cracked faces of the cementitious material for an extended period of time giving continuous aid to autogenous healing of the crack.<sup>14,15</sup> Secondly

the polymer tendons can be considered to act as an effective long-term prestressing system improving the performance of the cementitious structure.

### **Load Induced Stress**

This study also explored the viscoelastic behaviour of un-activated drawn PET when it is stressed by applied loading rather than by heat activation.

An investigation of this behaviour was undertaken through a second set of tests in which a screw tightening system was used to manually apply stress to a polymer specimen. This was carried out for initial stresses ranging from 4 MPa up to 20 MPa. Once the initial stress was reached, the screw tightening system was locked off to ensure a constant strain within the specimen. The force was monitored at 10 minute intervals using a 0.5 kN load cell for the duration of the test, typically 2 weeks. For these tests, a custom built rig was constructed, which may be seen in figure 6.



**Figure 6 – Experimental setup for manually applied stress relaxation tests**

A typical set of results for the above tests is shown in figure 7 for a case with an initial stress of 8 MPa. The stress on the specimen can be seen to fluctuate between a minimum of 7.41 MPa, and a maximum of 8.23 MPa. It can also be seen by observing the temperature and stress fluctuations together that there is a clear pattern of the stress reducing when the temperature increases. An analysis of this trend gave a Pearson's product-moment coefficient of -0.54. This means that there is a weak correlation between temperature increase and stress decrease, hence there must also be other factors causing further stress changes beyond that due to thermal movement. At this stage these further stress changes are assumed to be due to the viscoelastic relaxation of the material.

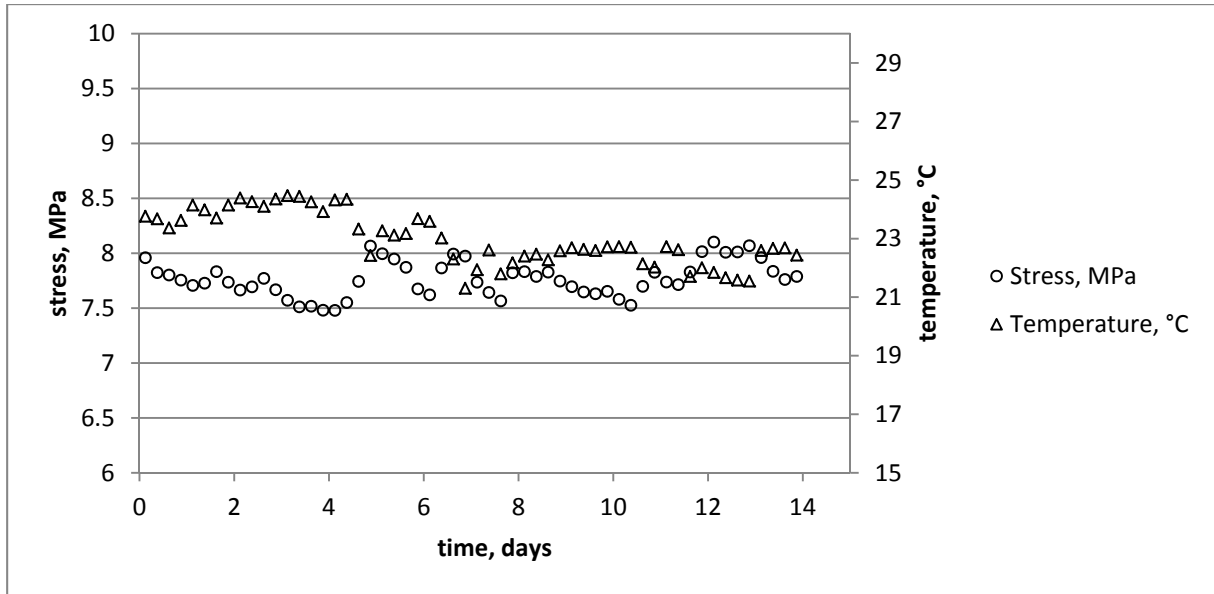


Figure 7 – Plot of stress vs time for a manually applied stress relaxation test, initial stress = 8 MPa

To investigate this assumption, the temperature change from the initial temperature was found and used to calculate the expected stress change due to thermal expansion or contraction of the specimen. This calculation was carried out based on the assumptions that the material behaves elastically and that the low temperature Young’s Modulus (6000 MPa) is applicable, the latter having been determined using the procedure described by Dunn et al<sup>4</sup>). A value of  $16 \times 10^{-6}$  was measured for the coefficient of thermal expansion hence the stress change due to any change in temperature,  $\Delta T$ , can be calculated from:

$$\Delta\sigma_T = \Delta T \cdot E_{TOT} \alpha_T \tag{1}$$

The original results were then modified by removing this stress change to reveal the underlying stress fluctuations. These modified results are shown in figure 8, which shows that the initial stress of 8 MPa gradually reduced to a plateau of approximately 7.6 MPa over a period of approximately 12 days. This trend was also observed in the other tests in this series in which (as mentioned above) the initial stress level varied from 4 to 20MPa. The time it took the stress to reach the plateau in these tests

varied from 12 to 14 days, and the specimens lost between 5 % and 10% of the initially applied stress.

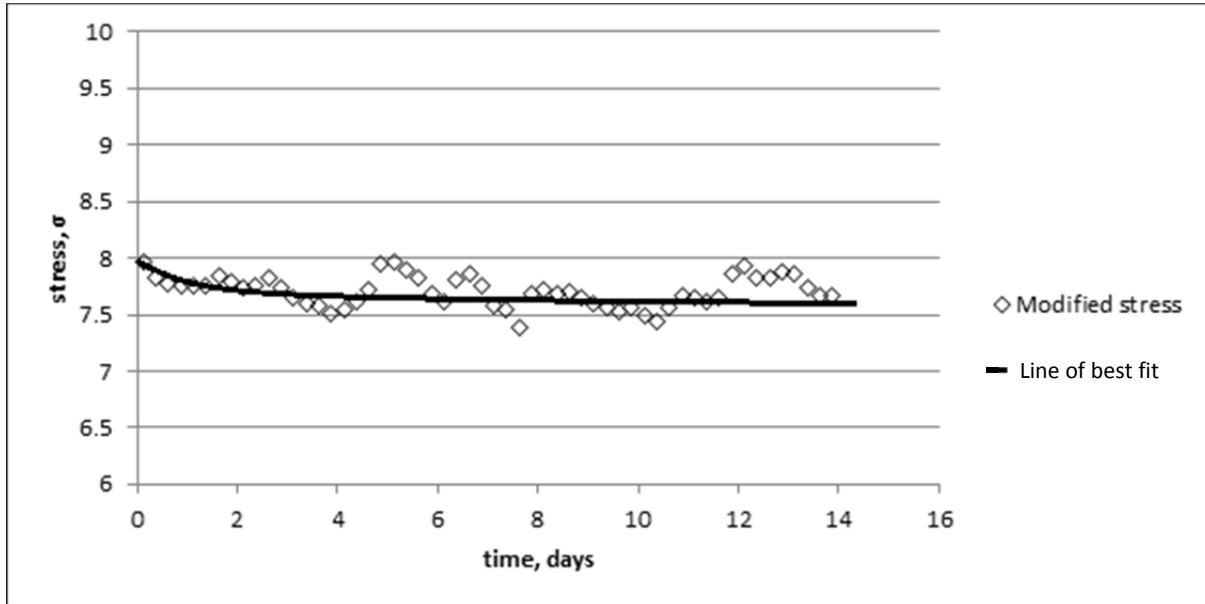


Figure 8 – Modified stress vs time for a manually applied stress relaxation test, initial stress = 8 MPa

Figure 9 presents the averaged result from 3 tests in which the stresses have been normalised to the pertinent initial stress. This plot confirms the trend that was earlier observed in the individual data sets.

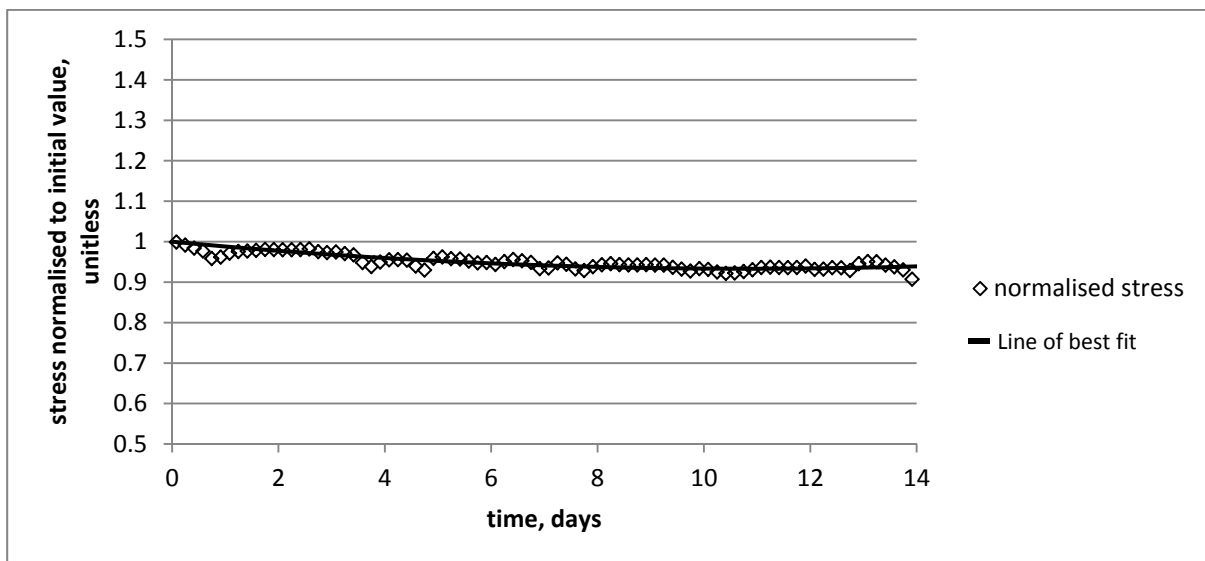


Figure 9 – Normalised modified stress vs time averaged across three manually applied relaxation tests

## CONSTITUTIVE MODEL

The following section describes the form of the newly developed constitutive model for the relevant behaviour of shape memory polymers. In this study, the model has only been applied to pre-drawn PET however, if properly calibrated, it is considered suitable for use with other shape memory polymers. The model is a modified version of that originally proposed by Dunn et al.<sup>4</sup> This model was capable of predicting the short term stress development under restrained shrinkage conditions. However, in order to be fully applicable to the LatConX system, a more comprehensive polymer model was required, capable of accurately simulating the long-term behaviour of the activated PET tendons. In addition, the thermodynamic issue referred to in the introduction to this paper also needed to be addressed. Modifications comprise the addition of a Maxwell arm in parallel with the existing Hookean spring element; this new arm takes account of the long-term creep (or relaxation) in the material. The thermal expansion element has also been applied to all three arms in the new model. The model is now able to predict the stress development under restrained shrinkage conditions in the same way as the previous model, as well as predicting long-term creep or stress relaxation behaviour induced by an applied stress or strain path respectively, including stress relaxation occurring subsequent to restrained shrinkage.

A representation of the proposed rheological model is shown in figure 10.

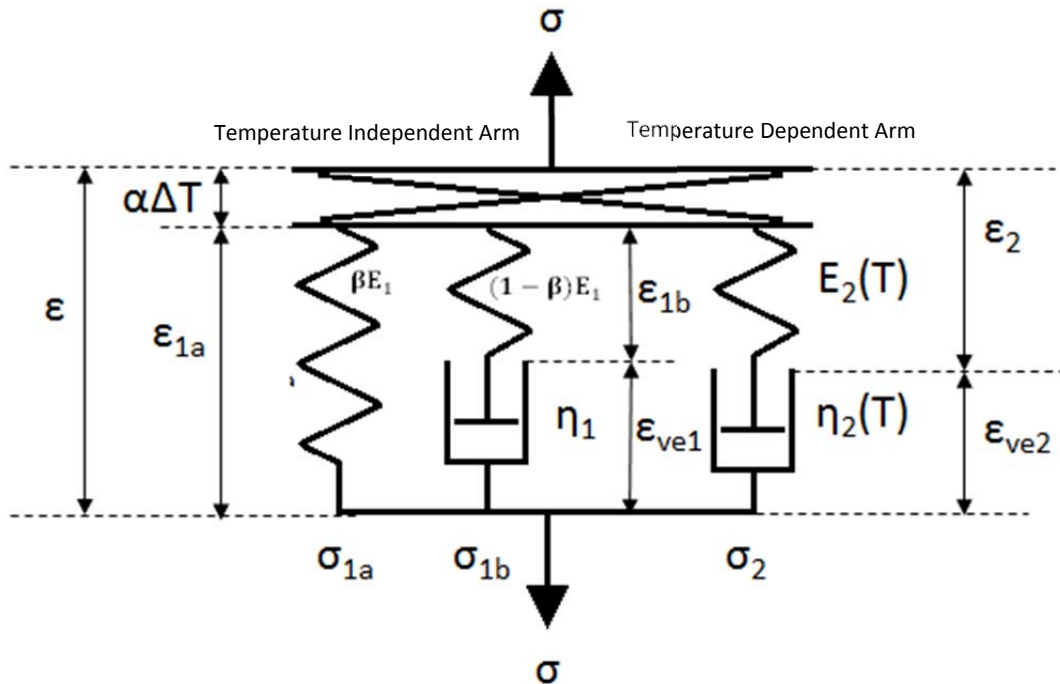


Figure 10 - Rheological representation of modified constitutive model

As shown in figure 10, the model consists of an elastic spring and two Maxwell elements in parallel. All three arms are in series with a thermal expansion element. In the second Maxwell element, both the Young's modulus of the spring and the viscosity of the dashpot are functions of temperature. This temperature dependent arm acts identically to the temperature dependent arm in the model of Dunn et al,<sup>4</sup> with the same temperature dependent functions for the material properties. The key development in this model is its ability to account for long-term viscoelastic behaviour of polymeric materials; this being achieved by the additional Maxwell arm in series with the thermal expansion element.

The total Young's modulus of the temperature independent arm,  $E_1$  is subdivided across the two elements by using a weighting factor,  $\beta$  ( $0 \leq \beta \leq 1$ ). The total stress is the sum of those in the arms:

$$\sigma_T = \sigma_{1a} + \sigma_{1b} + \sigma_2 \quad (2)$$

These stresses are given in the following equations:

$$\sigma_{1a} = \beta E_1 \cdot \varepsilon_{1a} \quad (3)$$

$$\sigma_{1b} = (1 - \beta)E_1 \cdot \varepsilon_{1b} = \eta_1 \cdot \dot{\varepsilon}_{ve1} \quad (4)$$

$$\sigma_2 = E_2(T) \cdot \varepsilon_2 = \eta_2 \cdot \dot{\varepsilon}_{ve2} \quad (5)$$

Where E is the Young's modulus of each spring,  $\eta$  is the viscosity of each dashpot, and each  $\varepsilon$  is the strain for the relevant element as displayed in figure 10.

The solution to equations (4) and (5) follows the standard procedure.<sup>16</sup>

$$\varepsilon_{vej} = \varepsilon_{\theta j} (1 - e^{-\Delta t/\tau}) + \varepsilon_{vej-1} \cdot e^{-\Delta t/\tau} \quad (6)$$

Where  $\Delta t$  is equal to  $t_j - t_{j-1}$ , and  $\theta$  is 0.5.

Making use of the solution above, the stresses at any time increment (j) may be written in terms of the total and viscous strains as follows:

$$\sigma_{1aj} = \beta E_1 \cdot [\varepsilon_j - \alpha_T \cdot (T_j - T_0)] \quad (7)$$

$$\sigma_{1bj} = (1 - \beta)E_1 \cdot [\varepsilon_j - \varepsilon_{ve1j} - \alpha_T \cdot (T_j - T_0)] \quad (8)$$

$$\sigma_{2j} = E_2(T) \cdot [\varepsilon_j - \varepsilon_{ve2j} - \alpha_T \cdot (T_j - T_0)] \quad (9)$$

Where  $T_0$  is the ambient temperature,  $\alpha_T$  is the coefficient of thermal expansion, and  $T_j$  is the temperature at time increment j.

As mentioned earlier, an issue with the thermodynamic validity of the model has been addressed in this modified version. The problem occurs when a decrease in the temperature applied causes an increase in the stress in arm 2 with no increase in the strain and no other energy source. This is due to the inversely proportional

relationship between temperature and Young's modulus. The solution to this problem is outlined below.

The stress in the temperature dependent arm is that shown in equation ( 10 ) (in which the contribution of thermal expansion has been removed for clarity):

$$\sigma_2 = E_2(T)(\varepsilon - \varepsilon_{ve2}) \quad (10)$$

In the absence of an associated thermodynamic source of energy, there should be no increase in stress due to the increase in stiffness alone i.e.:

$$\Delta\sigma_{\Delta E} = 0 \quad (11)$$

This is satisfied by the use of a small change in viscoelastic strain as follows:

$$\Delta\sigma_{\Delta T} = \Delta E_2(\varepsilon - \varepsilon_{ve2} - \Delta\varepsilon_{ve2}) + E_2(-\Delta\varepsilon_{ve2}) = 0 \quad (12)$$

Where:

$$\Delta E_2 = E_2(T_j) - E_2(T_{j-1}) \text{ but } \Delta E_2 > 0 \quad (13)$$

Rearranging gives:

$$\Delta\varepsilon_{ve2} = \frac{\Delta E_2(\varepsilon - \varepsilon_{ve2})}{E_2 + \Delta E_2} \quad (14)$$

This value of  $\Delta\varepsilon_{ve2}$  is then added to the current viscoelastic strain.

### **Model Parameters**

There are two new model parameters relating to the long-term Maxwell arm that need to be calibrated; the weighting factor  $\beta$ , and the relaxation time parameter  $\tau_1$  – from which the viscosity is calculated.

The permanent proportion of the locked in stress is controlled by  $\beta$ . The value of  $\beta$  can therefore be approximated by the relationship below:

$$\beta = \frac{\sigma_{plat\ exp}}{\sigma_{res}} \quad (15)$$

Where  $\sigma_{plat\ exp}$  is the average plateau stress, and  $\sigma_{res}$  is the value used in the model.  $\tau_1$  is then found by calibration. This essentially involves identifying the time at which the plateau stress is effectively first reached. Finally the viscosity of the long-term arm is given by:

$$\eta_1 = \tau_1 \cdot E_{1b} \quad (16)$$

It has been found that the values of the material parameters relating to the long-term arm vary with the age of the material. This is because the long-term relaxation processes are active from the time of manufacture and not just from the time of activation, which means that some of the locked-in stress is lost before any monitored process begins. This phenomenon was observed in the manually applied stress relaxation tests.

The 'low' and 'high' temperature Young's moduli and viscosities have been established following the basic approach described by Dunn et al.<sup>4</sup> The Young's moduli are the values consistent with short term stress excursion tests in which the loading rate is rapid enough for viscous effects to be minimal. The idealised variation of each of these properties with temperature is illustrated by Dunn et al.. Although the material used for the current tests was nominally the same as that used by Dunn

et al., the properties of this batch of material, given in Table 2 and 3, were found to be slightly different from those quoted by Dunn et al.<sup>4</sup>

### Model Validation

The model has been validated by comparison with an experimental data set. A specimen measuring 400 x 32 x 1.15 mm<sup>3</sup> was heated to 90°C, held at that temperature for a period of 10 minutes at which point the oven was turned off and the specimen monitored for a period of 124 days.

The above temperature path was applied to the newly developed model, using the material parameters from table 1, to simulate the experimental behaviour. The resulting experimental and numerical data are shown in figure 11 and figure 12.

**Table 1 – Numerical input values used to model hot stress relaxation**

Name	Symbol	Value
Ambient Temperature	$T_0$	22°C
Coefficient of thermal expansion	$\alpha_T$	$10^{-4.8}$
High temperature Young's modulus	$E_{TH}$	845 MPa
Low temperature Young's modulus	$E_{TOT}$	6000 MPa
Transition start temperature (Young's modulus)	$T_L$	70°C
Transition end temperature (Young's modulus)	$T_H$	120°C
Transition at the centre of the transition (Young's modulus)	$T_g$	95°C
Elastic modulus material parameter	b	3.3
Elastic modulus material parameter	d	1.2
Stress at drawing	$\sigma_{res}$	26.57 MPa
High temperature viscosity	$\eta_{2L}$	$1.575 \times 10^4$ P
Low temperature viscosity	$\eta_{2H}$	$3.122 \times 10^7$ P
Transition start temperature (viscosity)	$T_L$	30°C
Transition end temperature (viscosity)	$T_H$	90°C
Temperature at the centre of the transition (Viscosity)	$T_g$	60°C
Viscous material parameter	c	5
Viscous material parameter	f	0.1
Relaxation time parameter for long-term Maxwell arm	$\tau_1$	$2 \times 10^5$ s
Long-term Maxwell arm weighting factor	$\beta$	0.98

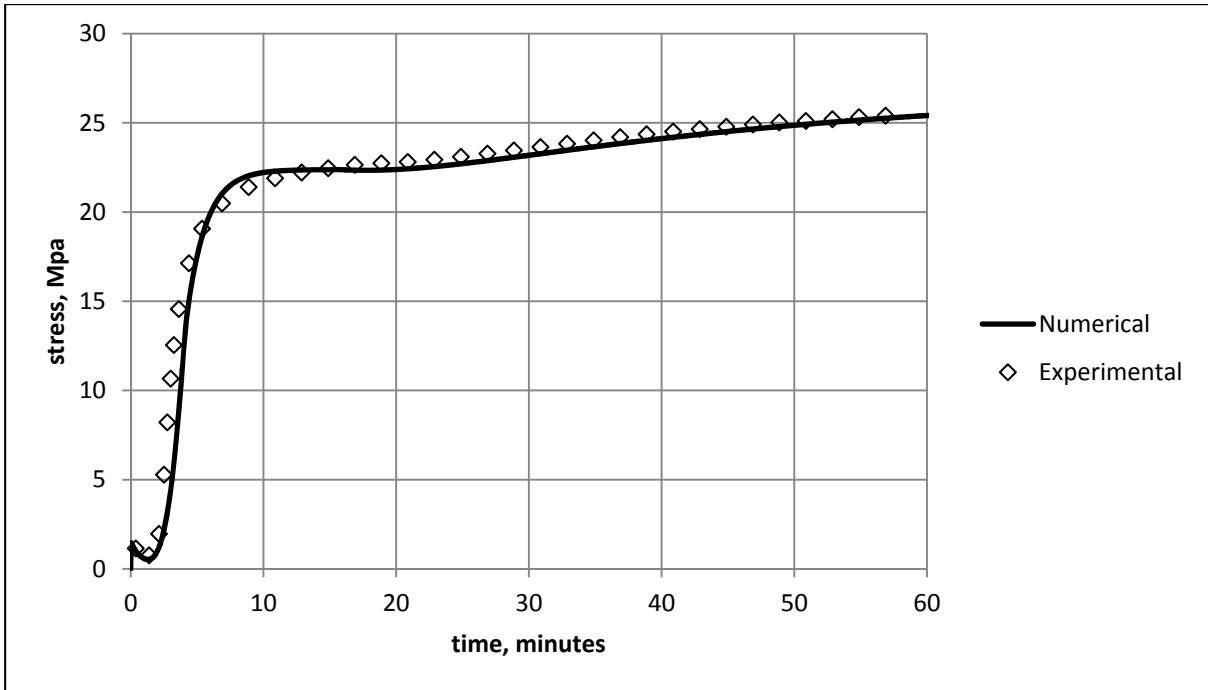


Figure 11 – Short term behaviour of rheological model compared to early experimental data

From figure 11 it is clear that the modified model is capable of reproducing the stress build up behaviour of this type in the same way as that of the original model of Dunn et al.<sup>4</sup>

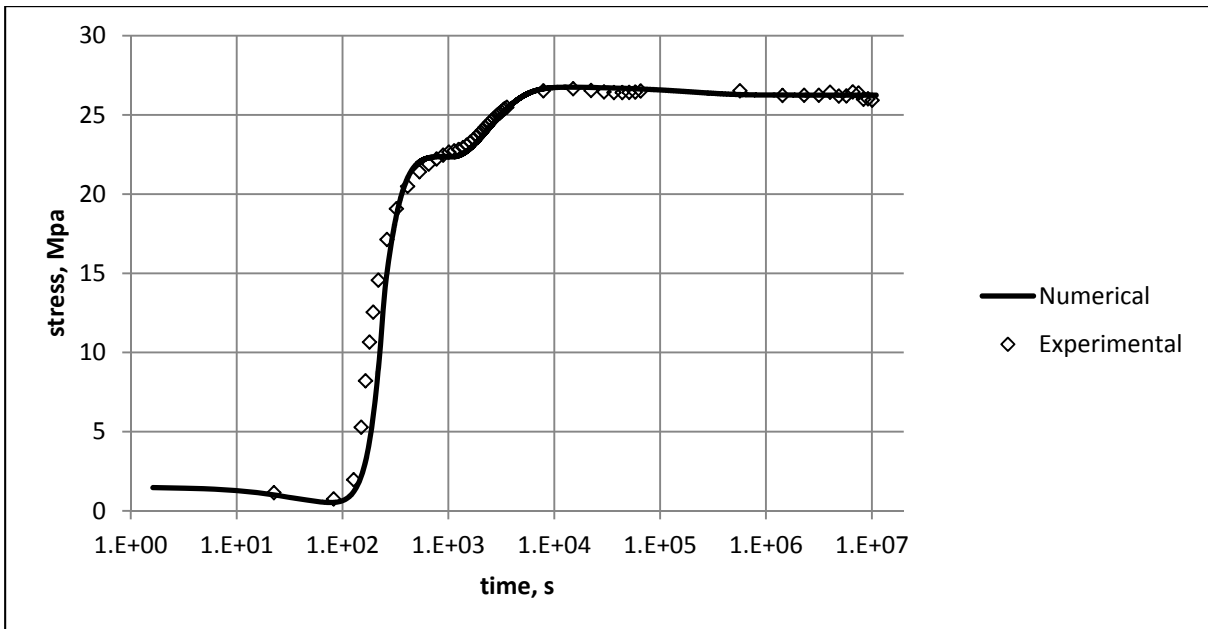


Figure 12 – Long-term behaviour of rheological model compared to full four month data set

Figure 12 shows the behaviour of the newly developed aspect of the model and indicates that there is very good agreement between the experimental behaviour and numerical prediction.

An ambient temperature stress relaxation data set has also been simulated using the model presented above. The values of the locked-in stress ( $\sigma_{res}$ ), the weighting factor ( $\beta$ ), and the relaxation time of the long-term arm ( $\tau_1$ ) are different from those used for the hot relaxation experiment due to their dependence on the age of the material from initial drawing.

The 8 MPa ‘ambient temperature stress relaxation test’ has been simulated using the material parameters displayed in table 2. In this test, a specimen measuring 400 x 32 x 0.92 mm<sup>3</sup> was loaded until an initial stress of 8 MPa was reached. The specimen was then held under constant displacement (and strain) and the stress monitored at 10 minute intervals for a period of 14 days.

Observations from these ambient temperature relaxation tests showed that between 5 % and 10% of any applied stress was lost to viscoelastic relaxation. However table 2 shows  $\beta$  taking the value of 0.97 suggesting that only 3% of the applied stress is allowed to relax. Closer inspection of the form of the model explains this apparent discrepancy. The 3% is applied to the stress on the temperature independent arm; this stress is considerably higher than the 8 MPa manually applied to the model as a whole since there is also the locked in stress of 26.6 MPa to consider. Thus 3% of the stress on the temperature independent arm equates to 10% of the overall stress on the model.

**Table 2 - Numerical input values used to model ambient temperature stress relaxation**

Name	Symbol	Value
------	--------	-------

Ambient Temperature	$T_0$	22°C
Coefficient of thermal expansion	$\alpha_T$	$10^{-4.8}$
Young's modulus at the high temperature	$E_{TH}$	845 MPa
Young's modulus at the low temperature	$E_{TOT}$	6000 MPa
Transition start temperature (Young's modulus)	$T_L$	70°C
Transition end temperature (Young's modulus)	$T_H$	120°C
Transition at the centre of the transition (Young's modulus)	$T_g$	95°C
Elastic modulus material parameter	b	3.3
Elastic modulus material parameter	d	1.2
Stress at drawing	$\sigma_{res}$	26.57 MPa
Viscosity at high temperature	$\eta_{2L}$	$1.575 \times 10^4$ P
Viscosity at low temperature	$\eta_{2H}$	$3.122 \times 10^7$ P
Transition start temperature (viscosity)	$T_L$	30°C
Transition end temperature (viscosity)	$T_H$	90°C
Temperature at the centre of the transition (Viscosity)	$T_g$	60°C
Viscous material parameter	c	5
Viscous material parameter	f	0.1
Relaxation time parameter for long-term Maxwell arm	$\tau_1$	$1 \times 10^6$ s
Long-term Maxwell arm weighting factor	$\beta$	0.97

Figure 13 shows model predictions for the case when ambient temperature stress relaxation behaviour is considered. Good agreement is observed between the experimental data and the model simulation. The model is capable of simulating both the stress decrease due to long-term relaxation of induced stress, and the stress increase due to the locked in stress gradually releasing over time. There is some discrepancy between the predicted and experimental stress fluctuations due to temperature changes but these are considered acceptable given the general level of variability of PET material behaviour.

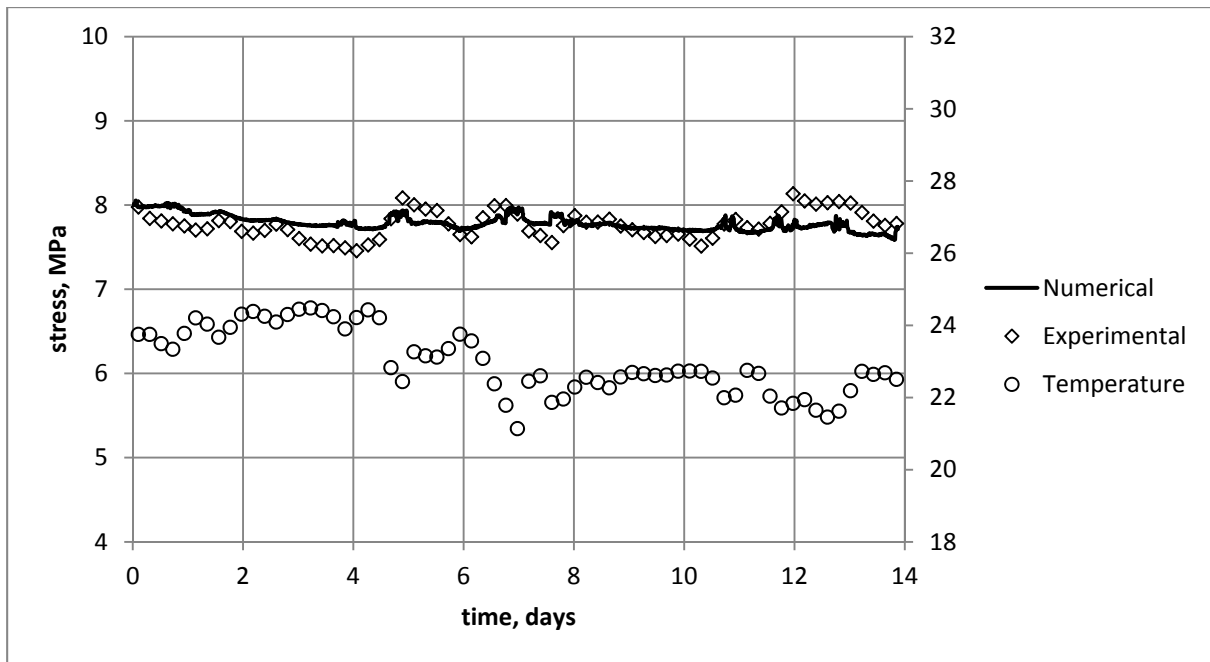


Figure 13 – Ambient temperature stress relaxation behaviour of model compared to 8 MPa data set

## CONCLUSIONS

An experimental and numerical study into the long-term stress relaxation behaviour of the shape memory polymer poly(ethylene terephthalate) has been presented. Stress relaxation of this material has been monitored over periods of time ranging from 2 weeks to 6 months. A numerical model has been described which is able to simulate the short and long-term thermo-mechanical behaviour of this material.

For the pre-drawn PET used in this study, the relaxation of thermally activated restrained shrinkage stresses is between 2 and 3 % of the peak stress. The stress relaxation time ( $\tau$ ) for unactivated samples is approximately 12 days, with the relaxation being between 5 % and 10% of the applied stress. These values are, however, considered to depend on the age of the material since drawing.

The new model is shown to accurately predict the stress relaxation behaviour of restrained PET specimens following heat activation, as well as the stress variation in specimens loaded in the pre activated state. The model is considered to be capable

of predicting similar behaviour in other shape memory polymer materials if properly calibrated.

### **Author Contributions**

The named authors are part of a team who undertook this work. The modus operandi of the group involves regular supervision sessions of the PhD investigator (Hazelwood) by Jefferson, Gardner and Lark. Gardner and Lark concentrated mostly on the experimental aspects, whilst Jefferson dealt with the modelling aspects. The input of each contributor to the ideas, results and text are considered sufficient for all to warrant inclusion as authors.

1. Jefferson, A.; Joseph, C.; Lark, R.; Isaacs, B.; Dunn, S.; Weager, B. *Cem Concr Res.* **2010**, 40(5), 795–801.
2. Pakula, T.; Trznadel, M. *Polymer.* **1985**, 26(7), 1011–8.
3. Morshedean, J.; Khonakdar, H. A.; Rasouli, S. *Macromol Theory Simul.* **2005**, 14(7), 428–34.
4. Dunn, S. C.; Jefferson, A. D.; Lark, R. J.; Isaacs, B. *J Appl Polym Sci.* **2011**, 120(5), 2516–26.
5. Liu, Y.; Gall, K.; Dunn, M. L.; Greenberg, A. R.; Diani, J. *Int J Plast.* **2006**, 22(2), 279–313.
6. Barot, G.; Rao, I. J. *Z Für Angew Math Phys.* **2006**, 57(4), 652–81.
7. Barot, G.; Rao, I. J.; Rajagopal, K. R. *Int J Eng Sci.* **2008**, 46(4), 325–51.
8. Qi, H. J.; Nguyen, T. D.; Castro, F.; Yakacki, C. M.; Shandas, R. *J Mech Phys Solids.* **2008**, 56(5), 1730–51.
9. Ward, I. M.; Sweeney, J. In *An introduction to the mechanical properties of solid polymers*; Chichester, West Sussex, England: Wiley; **2004**.
10. Wang, L. F.; Kuo, J. F.; Chen, C. Y. *Eur Polym J.* **1995**, 31(8), 769–73.
11. Almagableh, A.; Raju Mantena, P.; Alostaz, A. *J Appl Polym Sci.* **2010**, 115(3), 1635–41.
12. Drozdov, A. D. *Polymer.* **1998**, 39(6-7), 1327–37.
13. Xu, X.; Hou, J. *Mech Time-Depend Mater.* **2011**, 15(1), 29–39.
14. Ter Heide, N.; Schlangen, E. *First international conference on self healing materials* Springer, Dordrecht [Internet]. **2007** [cited 2013 May 23].
15. Isaacs, B.; Lark, R. J.; Jefferson, A. D.; Davies, R.; Dunn, S. *Struct Concr.* **2013**, 14(2), 138–47.
16. Simo, J. C.; Hughes, T. J. R. *Computational inelasticity*. New York: Springer; **1998**.